

Graph Neural Networks with Similarity-Navigated Probabilistic Feature Copying

Asela Hevaphige

School of Computing, Australian National University, Canberra, 2601, ACT, Australia

Abstract

Graph Neural Networks (GNNs) have demonstrated remarkable success across various graph-based tasks. However, they face some fundamental limitations: feature oversmoothing can cause node representations to become indistinguishable in deeper networks, they struggle to effectively manage heterogeneous relationships where connected nodes differ significantly, and they process entire feature vectors as indivisible units, which limits flexibility. We seek to address these limitations. We propose AxelGNN, a novel GNN architecture inspired by Axelrod’s cultural dissemination model that addresses these limitations through a unified framework. AxelGNN incorporates similarity-gated probabilistic interactions that adaptively promote convergence or divergence based on node similarity, implements trait-level copying mechanisms for fine-grained feature aggregation at the segment level, and maintains global polarization to preserve node distinctiveness across multiple representation clusters. The model’s bistable convergence dynamics naturally handle both homophilic and heterophilic graphs within a single architecture. Extensive experiments on node classification and influence estimation benchmarks demonstrate that AxelGNN consistently outperforms or matches state-of-the-art GNN methods across diverse graph structures with varying homophily-heterophily characteristics.

Keywords: graph neural networks, trait copying, oversmoothing, heterophily, feature segmentation

1. Introduction

Graph Neural Networks (GNNs) have been a cornerstone to many graph downstream tasks, such as node classification [1, 2], influence maximisation [3, 4], link prediction [5, 6], and community detection [7, 8]. This success can be attributed to their ability to effectively leverage the structural relationships within graph data,

which enables the learning of rich node representations that seamlessly integrate both node-level features and topological information through iterative message passing mechanisms [9].

Despite the strengths, GNNs have some notable limitations:

- **Feature Oversmoothing:** As GNNs stack more layers, node representations become increasingly similar to their neighbours, eventually converging to nearly identical embeddings across the entire graph [10]. This reduces the model’s ability to distinguish between different nodes and hurts performance, especially in downstream tasks that require deeper networks [11].
- **Inability to Handle Heterogeneous Relationships:** Traditional GNNs assume that connected nodes tend to have similar features and labels, known as the homophily assumption [12]. However, many real-world graphs exhibit heterophily, where connected nodes are actually dissimilar [13]. GNNs perform poorly on heterophilic graphs because their message-passing mechanism reinforces similarity between neighbours, which contradicts the underlying graph structure.
- **Monolithic Feature Treatment:** Existing GNNs treat node features as indivisible units during aggregation. The entire feature vector is processed as a single entity, without considering the individual importance or relationships between different feature dimensions. This prevents fine-grained feature-level interactions and limits the model’s ability to selectively aggregate specific aspects of neighboring node features.

We seek to address the limitations above. We observe that Axelrod’s cultural dissemination model [14] exhibits remarkable properties that directly correspond to the fundamental challenges in GNNs. The model’s dual convergence behavior naturally handles both homophilic and heterophilic relationships: similarity convergence (where neighboring agents become identical) mirrors beneficial feature sharing in homophilic graphs, while dissimilarity convergence (where neighboring agents become completely different) preserves node distinctiveness in heterophilic scenarios. Additionally, the model’s global polarization mechanism prevents the collapse to a single representation by maintaining multiple distinct cultural regions, directly addressing the oversmoothing problem. Finally, Axelrod’s trait-level copying mechanism operates on individual cultural dimensions rather than entire cultural vectors, providing a principled approach to fine-grained feature interactions that transcends monolithic feature treatment.

Motivated by these observations, we propose *AxelGNN*, a novel graph neural network architecture that incorporates the core principles of Axelrod’s cultural dissemination model into the neural message-passing framework. Our approach introduces similarity-gated interactions that adaptively promote convergence or divergence based on node similarity, implements trait-level copying mechanisms for fine-grained feature aggregation, and maintains global polarization to preserve node distinctiveness across multiple representation clusters. Our research contributions are summarised as follows:

- **Novel Formalisation:** We reformalize message-passing in GNNs as a feature dissemination model that has convergence guarantees with modeling homophily-heterophily dynamics and prevents oversmoothing via polarization mechanisms inspired by Axelrod’s cultural dissemination theory.
- **Novel GNN Architecture:** We propose *AxelGNN*, a novel graph neural network that incorporates similarity-gated interactions and trait-level copying mechanisms to address fundamental limitations in traditional GNN architectures.
- **Empirical Evaluation:** We conduct extensive experiments on node classification and influence estimation tasks, demonstrating that our approach achieves superior performance over state-of-the-art GNNs across diverse graph datasets with varying homophily-heterophily characteristics.

2. Related Work

2.1. Traditional GNNs

Graph Neural Networks have been increasingly used for diverse graph-related downstream tasks [15]. There have been many GNN types proposed with different inductive biases. Gilmer et al. [9] proposed one of the early GNNs based on the message-passing paradigm. Graph Convolutional Networks (GCNs) introduced a spectral-based perspective where convolution operations are defined in the spectral domain of graphs using the graph Laplacian matrix [16]. Graph Attention Networks (GATs) consider a learnable neighbourhood weighting mechanism for message-passing, going beyond traditional fixed, structure-based weighting schemes [17]. GraphSAGE is another GNN designed based on a sampling mechanism to enhance GNN’s scalability to large graphs [18]. However, these classical GNNs are known to work under the homophily assumption, thus cannot model heterogeneous relationships among neighbouring nodes, and are prone to oversmoothing.

2.2. *Heterophily-aware GNNs*

Pei et al[19] presented one of the early works that identified the performance degradation issue in GNNs under heterophilic data. Since then, researchers have proposed GNNs enhanced by various techniques to alleviate this limitation. Some of these works have proposed neighbourhood filtering to aggregate information from relevant neighbours selectively [20, 13, 21]. In contrast, some other works have introduced higher-order graph structures to capture multi-hop relationships that may be more informative than direct connections [12, 22, 23, 24]. There have been works utilising specific design decisions, such as tailored aggregation mechanisms [25, 26] and neighbourhood ordering [27], to enhance relevant information flow. These approaches aim to suppress noise flow in message passing. However, certain limitations still exist. First, many existing approaches cannot handle both homophilic and heterophilic data patterns within a single framework effectively. Most methods are specifically designed for either homophilic or heterophilic scenarios, limiting their practical applicability in real-world graphs that often exhibit mixed characteristics. Second, existing methods often lack the flexibility to adaptively determine when to emphasise local versus global information based on neighbourhood characteristics, resulting in suboptimal performance when the optimal aggregation strategy varies across different parts of the same graph.

2.3. *Oversmoothing in GNNs*

Oversmoothing in GNNs refers to the scenario where node features become increasingly similar and eventually indistinguishable in the embedding space as message passing iterations increase [10]. Existing works try to alleviate this issue through various mechanisms. Some works propose structural modifications, such as residual connections [28, 29, 30] and jumping knowledge mechanisms [31, 32], to retain initial representations of nodes to some extent, thus preventing the complete loss of node distinctiveness. Some other works introduced regularisation and normalisation techniques, such as dropout [33, 34, 35] and batch normalisation techniques [36, 37], to introduce controlled stochasticity and maintain feature diversity throughout the graph. Recently, researchers have used curvature-based methods to identify bottlenecks in graphs that lead to oversmoothing [38, 39, 40]. They also proposed graph rewiring and sampling methods to structurally correct these bottlenecks. However, most existing approaches still suffer from several limitations. First, they typically apply uniform treatments across the entire graph without considering local neighborhood characteristics, potentially over-correcting in regions where information sharing would be beneficial while under-correcting in areas where distinctiveness preservation is crucial. Second, many methods lack principled theoretical foundations for

determining when and how to prevent oversmoothing, often relying on heuristic solutions that may not generalise across different graph types and diverse downstream tasks. Finally, these approaches often fail to provide adaptive mechanisms that can simultaneously handle both homophilic regions where controlled smoothing is desirable and heterophilic regions where preservation of differences is essential within the same graph structure.

2.4. Novelty of Our work

Our AxelGNN introduces a novel paradigm that fundamentally differs from existing heterophily and oversmoothing GNNs by providing a unified framework grounded in Axelrod’s cultural dissemination theory. Unlike existing approaches that are typically designed for either homophilic or heterophilic scenarios, AxelGNN adaptively handles both patterns within a single architecture through similarity-gated probabilistic interactions and bistable convergence dynamics. The method’s trait copying mechanism breaks the monolithic feature assumption by operating on grouped feature segments rather than entire feature vectors. This enables fine-grained modeling of complex relationships where different feature dimensions may exhibit varying similarity patterns. This approach naturally prevents oversmoothing through global polarization while maintaining selective information flow, addressing fundamental limitations of existing methods that apply uniform treatments across diverse graph regions.

3. Background and Motivation

In this section, we present Axelrod’s model of cultural dissemination and discuss its implications for addressing the gaps in GNNs.

3.1. Axelrod’s Cultural Dissemination Model

The model simulates cultural dissemination on an $L \times L$ grid, where each cell represents an agent with a cultural vector. Each agent i has a cultural vector $\mathbf{v}^i = (v_1^i, v_2^i, \dots, v_f^i)$ with f cultural dimensions (i.e., traits), where each trait v_j^i can take q possible discrete values from $\{0, 1, \dots, q - 1\}$. Agents start with random trait assignments.

The cultural similarity between two agents i and j is defined as:

$$s_{ij} = \frac{|\{k : v_k^i = v_k^j\}|}{f} \tag{1}$$

where $s_{ij} \in [0, 1]$ represents the fraction of matching traits between agents i and j .

At each time step, an active agent k and a passive neighbour r are selected randomly. They interact with probability s_{kr} , where s_{kr} is their cultural similarity. If interacting, k copies one of r 's differing traits at random. The system reaches equilibrium when all neighbouring pairs are either identical ($s_{kr} = 1$) or completely dissimilar ($s_{kr} = 0$). The pseudo-code of the Axelrod model is depicted in Algorithm 1.

Algorithm 1: Axelrod Cultural Dissemination Model

```

1: Input: Grid size  $L$ , number of features  $f$ , number of traits per feature  $q$ 
2: Initialization:
3: for each agent  $i$  in  $L \times L$  grid do
4:   Initialize cultural vector  $\mathbf{v}^i = (v_1^i, v_2^i, \dots, v_f^i)$ 
5:   for  $j = 1$  to  $f$  do
6:      $v_j^i \leftarrow$  random integer from  $\{0, 1, \dots, q - 1\}$ 
7:   end for
8: end for
9: Main Evolution Loop:
10: repeat
11:   Select random agent  $k$  from grid
12:   Select random neighbor  $r$  of  $k$ 
13:   Compute similarity:  $s_{kr} = |\{i : v_i^k = v_i^r\}|/f$ 
14:   if random number from  $[0, 1) < s_{kr}$  then
15:      $D \leftarrow \{i : v_i^k \neq v_i^r\}$  {Differing features}
16:     if  $D \neq \emptyset$  then
17:       Select  $d \leftarrow$  random element from  $D$ 
18:        $v_d^k \leftarrow v_d^r$  {Cultural trait adoption}
19:     end if
20:   end if
21: until cultural equilibrium reached
22: Termination: Equilibrium when for all adjacent agents  $(k, r)$ :
23:   Either  $\mathbf{v}^k = \mathbf{v}^r$  (identical) or  $s_{kr} = 0$  (dissimilar)

```

3.2. Convergence and Polarisation in Axelrod Model

The Axelrod model exhibits two interesting properties in terms of convergence. The model achieves local convergence among neighbours while having global polarisation. Below, we formally define these concepts and explain how the Axelrod model achieves them.

3.2.1. Local Convergence

We first define the local convergence property of the Axelrod model, which exhibits bistable dynamics. In this model, neighbouring agents cannot maintain intermediate levels of similarity. Instead, they converge either to complete cultural alignment or to total separation.

Definition 1 (Local Convergence). *For neighboring agents i and j , local convergence occurs when $\lim_{t \rightarrow \infty} s_{ij}(t) \in \{0, 1\}$, encompassing:*

- *Similarity convergence: $s_{ij} \rightarrow 1$ (identical cultures)*
- *Dissimilarity convergence: $s_{ij} \rightarrow 0$ (disjoint cultures)*

The bistable behaviour of the Axelrod model emerges from the similarity-dependent interaction mechanism, where agents with higher similarity interact more frequently and subsequently become more alike, while agents with lower similarity interact less frequently and eventually lose all common traits through competing influences from their respective neighbourhoods.

3.2.2. Global Polarization

We define the global polarization property of the Axelrod model as a critical equilibrium state in which the system divides into distinct cultural regions. These regions maintain a permanent separation due to the absence of shared traits between neighboring groups.

Definition 2 (Global Polarization). *Global polarization occurs when the system partitions into $K \geq 2$ cultural groups $\{G_1, \dots, G_K\}$ where each G_k is a non-empty subset of agents for $k = 1, \dots, K$, such that:*

$$s_{ij} = 0 \quad \forall i \in G_k, j \in G_m, k \neq m, \text{ where } i \text{ and } j \text{ are neighboring agents}$$

Global polarization of the Axelrod model emerges through progressive boundary sharpening. As local regions homogenize, they lose the trait overlap that enables cross-regional interaction. When $s_{ij} = 0$ between neighboring regions, interaction probability drops to zero, creating permanent cultural boundaries. The same similarity-based mechanism that unifies local neighborhoods simultaneously destroys the connectivity necessary for global consensus, fragmenting the system into isolated cultural domains.

3.3. Motivation: Addressing Homophily, Heterophily, and Oversmoothing in GNNs

The Axelrod model’s convergence properties directly map to fundamental challenges in graph neural networks, providing a principled framework for diverse downstream tasks.

3.3.1. Direct Mapping to Homophily/ Heterophily Paradigms

The dual local convergence states in the Axelrod model naturally correspond to homophily-heterophily downstream task scenarios:

- Homophily \leftrightarrow Local Similarity Convergence: In homophilic graphs where similar nodes are connected, the model promotes $s_{ij} \rightarrow 1$, enabling beneficial feature sharing and alignment between neighboring nodes of the same class
- Heterophily \leftrightarrow Local Dissimilarity Convergence: In heterophilic graphs where dissimilar nodes are connected, the model drives $s_{ij} \rightarrow 0$, preserving node distinctiveness and preventing harmful feature averaging between nodes of different classes

3.3.2. Global Polarization Prevents Oversmoothing

Traditional GNNs suffer from oversmoothing because all nodes converge to a single representation as depth increases [41]. The Axelrod model’s global polarization mechanism directly addresses this fundamental limitation. Rather than converging to a single global minimum, the system fragments into multiple cultural regions, naturally preserving multiple distinct node representations. The formation of stable cultural boundaries with $s_{ij} = 0$ between regions prevents different node classes from collapsing into identical representations. Furthermore, similarity-gated interactions ensure that information flows within semantically coherent regions while maintaining separation between different classes, enabling selective information flow that preserves node distinctiveness throughout the learning process.

4. Methodology

In this section, we propose a novel GNN architecture called AxelGNN based on the Axelrod cultural dissemination model. We start by providing preliminaries and then offer a comprehensive explanation of each component.

4.1. Preliminaries

Let $G = (V, E)$ be an undirected graph where V and E are the node and edge sets, respectively. Each node $v \in V$ has neighborhood $N(v) = \{u | (u, v) \in E\}$. Further, $x_v \in \mathbb{R}^d$ represents initial node features of node v with the feature dimension of d . In each GNN layer, the node features would represent a transformation with respect to the node features in the previous layer and the graph structure. We denote the node feature of v in layer l to be $x_v^l \in \mathbb{R}^{d^{(l)}}$ where $d^{(l)}$ is the feature dimensionality at layer l .

4.2. Interaction Probability Computation

We start by computing the interaction probability for each neighbouring node pair. For layer l , node features are first transformed via a learnable function:

$$\mathbf{h}_u^{(l)} = \mathbf{W}^{(l)} \mathbf{x}_u^{(l-1)} + \mathbf{b}^{(l)} \quad (2)$$

where $\mathbf{W}^{(l)} \in \mathbb{R}^{d^{(l-1)} \times d^{(l)}}$, and $\mathbf{b}^{(l)} \in \mathbb{R}^{d^{(l)}}$ are matrices with learnable parameters. Feature similarity between nodes v and u is computed as:

$$s_{vu}^{(l)} = \frac{\mathbf{h}_v^{(l)} \cdot \mathbf{h}_u^{(l)}}{\|\mathbf{h}_v^{(l)}\|_2 \|\mathbf{h}_u^{(l)}\|_2 + \epsilon} \quad (3)$$

Note that ϵ is a small constant employed for numerical stability (i.e., to avoid division by zero if either vector has zero norm). The interaction probability between nodes v and u at layer l is computed as:

$$p_{vu}^{(l)} = f(s_{vu}^{(l)}) \quad (4)$$

where $f : [-1, 1] \rightarrow [0, 1]$ is a monotonically increasing interaction function that maps feature similarity to interaction probability. We implement this interaction function using a sigmoid (σ) formulation that provides interpretable and learnable control over interaction dynamics:

$$f(s) = \sigma(\beta \cdot (s - \theta)) \quad (5)$$

Then, the complete interaction probability becomes:

$$p_{vu}^{(l)} = f(s_{vu}^{(l)}) = \sigma(\beta \cdot (s_{vu}^{(l)} - \theta)) \quad (6)$$

where β is the intensity parameter and θ is threshold parameter. This functional form was chosen for several important reasons. The sigmoid function naturally provides bounded output in the range $(0, 1)$, ensuring valid probability values, while maintaining monotonic behavior that preserves similarity ordering. The differentiability of the sigmoid function throughout its domain enables effective gradient-based learning during neural network training. The threshold parameter $\theta \in [-1, 1]$ determines the minimum similarity required for meaningful interaction. Higher values establish restrictive thresholds suitable for heterophilic graphs, while lower values create permissive thresholds that accommodate homophilic structures. The intensity parameter $\beta \in \mathbb{R}^+$ controls the steepness of the sigmoid transition, regulating the trade-off between information flow and node diversity preservation. Small values promote broad information exchange but risk oversmoothing, while large values create selective interactions that maintain node distinctiveness.

4.3. Message Passing and Aggregation

Feature influence from neighbor u to node v at layer l is computed as:

$$m_{u \rightarrow v}^l = p_{uv}^l \cdot h_u^l \quad (7)$$

Node v aggregates messages from its neighborhood $\mathcal{N}(v)$:

$$a_v^l = \frac{1}{|\mathcal{N}(v)|} \sum_{u \in \mathcal{N}(v) \cup \{v\}} m_{u \rightarrow v}^l \quad (8)$$

In the next step, we implement the trait copying mechanism in the AxelGNN. We group traits into segments of size s and compute copying probabilities at the group level. Let $C = \lceil d^{(l)}/s \rceil$ be the number of groups. For each group j , a copying probability is computed using a neural network $\phi_j : \mathbb{R}^{2s} \rightarrow \mathbb{R}^s$:

$$\mathbf{c}_{v,j} = \phi_j([\mathbf{h}_v^l[js : \min((j+1)s, d^{(l)})], \mathbf{a}_v^l[js : \min((j+1)s, d^{(l)})]]) \quad (9)$$

The updated node representation combines the original and aggregated values for each group:

$$\begin{aligned} \mathbf{x}_v^l[js : \min((j+1)s, d^{(l)})] &= \mathbf{c}_{v,j}^l \odot \mathbf{a}_v^l[js : \min((j+1)s, d^{(l)})] \\ &\quad + (\mathbf{1} - \mathbf{c}_{v,j}^l) \odot \mathbf{h}_v^l[js : \min((j+1)s, d^{(l)})] \end{aligned} \quad (10)$$

where \odot denotes element-wise multiplication and the group size s controls the granularity of trait copying.

4.4. A Simplified Variant

In this section, we present a lightweight variant of AxelGNN called AxelGNN_{Sim}. This variant replaces the group-specific neural networks from Eq. 6 with simple learnable weights, reducing the complexity of AxelGNN by a significant margin.

Instead of computing copying probabilities using group-specific neural networks ϕ_j for each group, AxelGNN_{Sim} maintains simple learnable parameters at the group level. Using the same grouping structure with $C = \lceil d^{(l)}/s \rceil$ groups, we maintain learnable parameters $\mathbf{W}_{\text{group}}^{(l)} \in \mathbb{R}^{C \times s}$ and compute group-specific copying probabilities:

$$\mathbf{C}^{(l)} = \sigma(\mathbf{W}_{\text{group}}^{(l)}) \quad (11)$$

where $\sigma : \mathbb{R}^{C \times s} \rightarrow (0, 1)^{C \times s}$. For group j containing traits $[js, \min((j+1)s, d^{(l)})]$, the copying probabilities are:

$$\mathbf{c}_j^{(l)} = \mathbf{C}^{(l)}[j, : (\text{group_size})] \quad (12)$$

The node update rule applies group-specific copying:

$$\begin{aligned} \mathbf{x}_v^{(l)}[js : \min((j+1)s, d^{(l)})] &= \mathbf{c}_j^{(l)} \odot \mathbf{a}_v^{(l)}[js : \min((j+1)s, d^{(l)})] \\ &+ (\mathbf{1} - \mathbf{c}_j^{(l)}) \odot \mathbf{h}_v^{(l)}[js : \min((j+1)s, d^{(l)})] \end{aligned} \quad (13)$$

This simplification eliminates the need for group-specific neural networks ϕ_j while maintaining the same grouped copying structure. The group size hyperparameter s continues to control the granularity of trait copying.

The high-level architectural workflow in AxelGNN is depicted in Figure 1.

4.5. Comparison of AxelGNN with Axelrod Cultural Dissemination Model

In this section, we compare different components of the Axelrod cultural dissemination model with our AxelGNN architecture. This comparison demonstrates that our GNN offers a robust neural approximation of the Axelrod model by retaining its key components, thereby extending its stochastic and discrete nature into a differentiable and continuous setting, which is required for learning tasks.

| Component | Axelrod Model | AxelGNN |
|------------------|-------------------------------------|--|
| Mechanism | Discrete copying | Neural gating |
| Learning | Static rules | Trainable parameters |
| Traits | Discrete features | Continuous features |
| Similarity | Trait overlap | Feature similarity |
| Interaction Rule | Probabilistic | Learned function |
| Trait Adoption | Copy one random trait from neighbor | Weighted aggregation + feature copying |
| Scope | Local | Local |
| Dynamics | Stochastic and agent-based | Deterministic and differentiable |

Table 1: Axelrod Model vs AxelGNN Comparison

4.6. Complexity Analysis

The computational complexity varies between the two variants of our model. In AxelGNN, the computational complexity at layer l is:

$$\mathcal{O}(|V|d^{(l-1)}d^{(l)} + |E|d^{(l)} + |V| \cdot C \cdot s \cdot k)$$

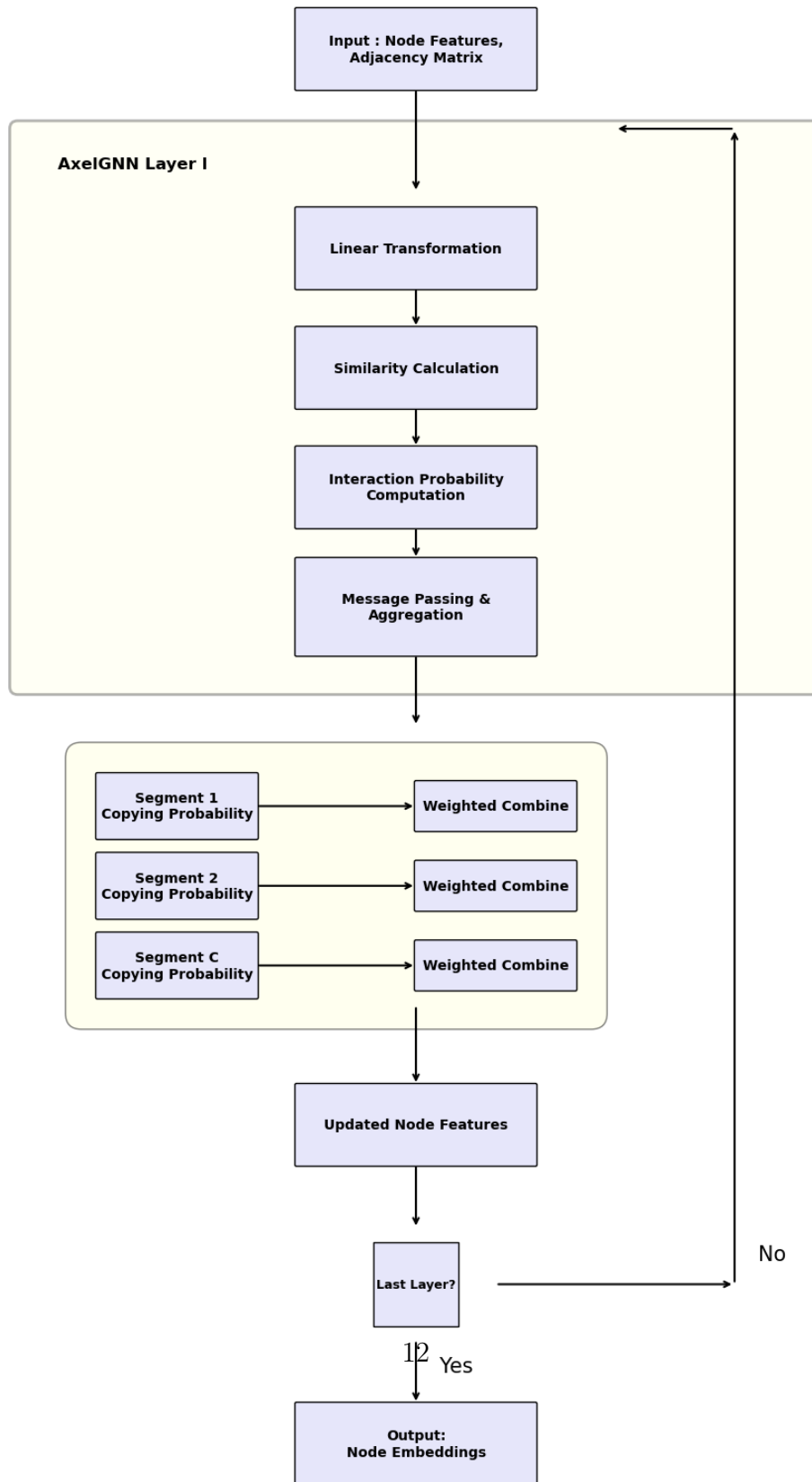


Figure 1: AxelGNN architecture overview showing the layer-wise processing flow with segment-based aggregation and iterative refinement through multiple layers.

where $C = \lceil d^{(l)}/s \rceil$ is the number of groups, s is the group size, and k represents the hidden dimension of the group-specific neural networks ϕ_j . The term $|V| \cdot C \cdot s \cdot k$ is associated with calculating group-specific copying probabilities.

AxelGNN_{sim} simplifies the complexity of AxelGNN to:

$$\mathcal{O}(|V|d^{(l-1)}d^{(l)} + |E|d^{(l)})$$

which removes the expensive group-specific neural network computations. The parameter count for copying mechanisms is reduced from $C \times k$ neural network parameters per group to $C \times s$ simple weights, achieving a significant speedup factor of approximately $|V|k$ in the computation of copying probabilities. The choice of group size s becomes a key hyperparameter that allows us to tune the trade-off between model expressiveness and computational efficiency. This simplification makes AxelGNN_{sim} particularly well-suited for large-scale graphs where computational efficiency is crucial.

5. Experimental Design

5.1. Downstream tasks

To evaluate AxelGNN’s ability to model complex relationships, we employ two downstream tasks: node classification and influence estimation.

Node Classification.: Node classification aims to predict a class label for each node in the graph [1]. GNN modeling of complex relationships is essential for node classification, as some real-world datasets exhibit heterophily, making traditional aggregation ineffective. Moreover, oversmoothing results in loss of node discriminability, making them indistinguishable.

Influence Estimation.: Influence estimation is a node regression task that predicts the activation probability for each node in a graph. Given a set of seed nodes that are initially activated and an influence diffusion model, the goal is to predict the likelihood that each node will become active after the diffusion process ends [11]. This task has significant real-world applications, including viral marketing campaigns, epidemic modelling, social media information spread, and technology adoption forecasting. Traditional algorithms designed for this task rely on computationally expensive Monte Carlo simulations that run thousands of diffusion scenarios to estimate probabilities, making them impractical for large networks or real-time applications [11]. GNN-based methods can directly learn these probabilities from graph structure, reducing computational complexity from exponential to linear. Modeling complex

relationships is crucial in influence estimation because diffusion involves multi-hop dependencies where a node’s activation depends on cascading effects through longer paths and community structures, not just immediate neighbors. Avoiding over-smoothing is particularly critical here since diffusion estimation typically requires GNNs with more than 2-4 layers to capture multi-step propagation dynamics.

5.2. Datasets

For node classification, we employ eight datasets consisting of both homophilic and heterophilic datasets. Homophilic datasets include Cora, Citeseer, and Pubmed from CitationFull benchmark [42], and heterophilic datasets include Cornell, Film, Wisconsin, and Texas from WebKB [19], as well as Penn94 from LINKX [43]. For influence estimation, we employ four real-world datasets, namely, Jazz, Cora-ML, Network Science, and Power Grid [44, 45]. The dataset statistics for node classification and influence estimation are provided in Table 2 and Table 3, respectively.

| Datasets | Nodes | Edges | Features | Classes | Homophily Ratio |
|-----------|--------|-----------|----------|---------|-----------------|
| Cora | 2708 | 5278 | 1433 | 7 | 0.81 |
| Pubmed | 19,717 | 44,327 | 500 | 3 | 0.80 |
| Citeseer | 3327 | 4676 | 3703 | 6 | 0.74 |
| Penn94 | 41,554 | 1,362,229 | 5 | 2 | 0.47 |
| Cornell | 183 | 280 | 1703 | 5 | 0.30 |
| Film | 7600 | 26,752 | 931 | 5 | 0.22 |
| Wisconsin | 251 | 466 | 1,703 | 5 | 0.21 |
| Texas | 183 | 295 | 1703 | 5 | 0.11 |

Table 2: Dataset Statistics - Node Classification

| Dataset | Nodes | Edges |
|-----------------|-------|--------|
| Jazz | 198 | 2,742 |
| Cora-ML | 2,810 | 7,981 |
| Network Science | 1,565 | 13,532 |
| Power Grid | 4,941 | 6,594 |

Table 3: Dataset Statistics - Influence Estimation

5.3. Baselines

For node classification, we utilize traditional GNNs such as GCN [16], GAT [17], and GraphSAGE [18]. Additionally, we include state-of-the-art models that are designed to address heterophily and alleviate oversmoothing in graph neural networks

(GNNs), including MixHop [46], GCNII [47], H2GCN [12], WRGAT [48], GPRGNN [49], GGCN [50], ACM-GCN [13], LINKX [43], GloGNN++ [51], PCNet [24], and DirGNN [52] as our baselines.

For influence estimation, we compare our approach with traditional GNNs such as GCN [16], GAT [17], and GraphSAGE [18]. Additionally, we incorporate GNN methods that are specifically designed for influence estimation and dynamic prediction tasks, including DeepIS [11], DeepIM [53], GLIE [54], and UniGO [55] as our baselines.

5.4. Evaluation Settings

For node classification, we employ a training/validation/testing split of 60/20/20 following work in literature [48, 24]. For AxelGNN variants and baselines, we report the mean and standard deviation of accuracy over 10 random initialisations.

We evaluate influence estimation over two diffusion models: Linear Threshold (LT) [56], and Susceptible-Infected-Susceptible (SIS) [57]. LT is a progressive diffusion model where nodes become activated when the weighted influence from their activated neighbors exceeds a predefined threshold, and SIS is a non-progressive diffusion model where nodes can transition between susceptible and infected states, allowing previously infected nodes to become susceptible again. We follow the experimental setup and dataset splits provided by Ling et al. [53]. In our experiments, we randomly select 10% of nodes as the initial activation set for each diffusion scenario, use 10-fold cross-validation and report both the mean and standard deviation of Mean Absolute Error (MAE).

For baseline results, we employ results reported in previous papers that have the same experimental setups. When such results are not available, we run the baseline methods using the hyperparameter settings specified in their original papers and report the results to ensure fair comparison.

5.5. Model Hyperparameters

We employ grid search [58] to find the best hyperparameters for AxelGNN variants. We use different numbers of layers $\in \{1, 2, 3, 4\}$, learning rates $\in \{1e^{-3}, 5e^{-3}, 1e^{-2}\}$, weight decay values $\in \{5e^{-4}, 1e^{-1}\}$, dropout rates $\in \{0.1, 0.4, 0.5\}$, hidden dimensions $\in \{32, 64, 256\}$, and segment sizes (s) $\in \{4, 8, 16\}$. Models were trained for up to 1000 epochs for node classification and 200 epochs for influence estimation. Further, we employ the Adam algorithm [59] for model optimization.

5.6. System Resources, and Implementation Details

We conduct all our experiments on a Linux server equipped with an Intel Xeon W-2175 2.50 GHz processor across 28 cores, with an NVIDIA RTX A6000 GPU and

512 GB of RAM. For implementation, we use the Python programming language [60] with PyTorch 2.3.1 as the core framework, along with the following libraries: torchvision 0.18.1, torchaudio 2.3.1, torch-geometric 2.7.0, torch-cluster 1.6.3, torch-scatter 2.0.9, and torch-sparse 0.6.18 [61].

6. Results, and Discussion

6.1. RQ1: How do AxelGNN variants compare to state-of-the-art GNNs for node classification and influence estimation benchmarks?

To evaluate the effectiveness of our proposed AxelGNN variants, we conduct comprehensive experiments comparing their performance against state-of-the-art GNN methods across node classification and influence estimation benchmarks.

6.1.1. Node Classification

| Dataset | Cora | Citeseer | Pubmed | Texas | Actor | Cornell | Wisconsin | Penn94 |
|------------------------|-------------------------|-------------------------|-------------------------|-------------------------|-------------------------|-------------------------|-------------------------|-------------------------|
| GCN | 86.98 \pm 1.27 | 76.50 \pm 1.36 | 88.42 \pm 0.50 | 55.14 \pm 5.16 | 27.32 \pm 1.10 | 60.54 \pm 5.30 | 51.76 \pm 3.06 | 82.47 \pm 0.27 |
| GAT | 87.30 \pm 1.10 | 76.55 \pm 1.23 | 86.33 \pm 0.48 | 52.16 \pm 6.63 | 27.44 \pm 0.89 | 61.89 \pm 5.05 | 49.41 \pm 4.09 | 81.59 \pm 0.55 |
| GraphSAGE | 86.90 \pm 1.04 | 76.04 \pm 1.30 | 88.45 \pm 0.50 | 82.43 \pm 6.14 | 34.23 \pm 0.99 | 75.95 \pm 5.01 | 81.18 \pm 5.56 | 80.94 \pm 0.66 |
| MixHop | 87.61 \pm 0.85 | 76.26 \pm 1.33 | 85.31 \pm 0.61 | 77.84 \pm 7.73 | 32.22 \pm 2.34 | 73.51 \pm 6.34 | 75.88 \pm 4.90 | 83.40 \pm 0.71 |
| GCNII | 88.37 \pm 1.25 | 77.33 \pm 1.48 | 90.15 \pm 0.43 | 77.57 \pm 1.83 | 37.44 \pm 1.30 | 77.86 \pm 3.79 | 80.39 \pm 3.40 | 82.92 \pm 0.59 |
| H2GCN | 87.87 \pm 1.20 | 77.11 \pm 1.57 | 89.49 \pm 0.38 | 84.86 \pm 2.73 | 35.70 \pm 4.00 | 82.70 \pm 5.28 | 87.65 \pm 4.98 | 81.31 \pm 0.60 |
| WRGAT | 88.20 \pm 1.26 | 76.81 \pm 1.89 | 88.52 \pm 0.99 | 83.62 \pm 6.50 | 36.33 \pm 1.77 | 81.62 \pm 3.90 | 86.98 \pm 3.78 | 74.32 \pm 1.63 |
| GPRGNN | 87.95 \pm 1.18 | 77.13 \pm 1.67 | 87.54 \pm 0.38 | 78.38 \pm 4.36 | 34.63 \pm 1.22 | 80.27 \pm 8.11 | 82.94 \pm 4.21 | 81.38 \pm 0.16 |
| GGCN | 87.95 \pm 1.05 | 77.14 \pm 1.45 | 89.15 \pm 0.37 | 84.86 \pm 4.55 | 37.54 \pm 1.56 | 85.68 \pm 6.63 | 86.86 \pm 3.22 | OOM |
| ACM-GCN | 87.91 \pm 0.95 | 77.32 \pm 1.70 | 90.00 \pm 0.52 | 87.84 \pm 4.40 | 36.28 \pm 1.09 | 85.14 \pm 6.07 | 88.43 \pm 3.22 | 82.52 \pm 0.96 |
| LINKX | 84.64 \pm 1.13 | 73.19 \pm 0.99 | 87.86 \pm 0.77 | 74.60 \pm 8.37 | 36.10 \pm 1.55 | 77.84 \pm 5.81 | 75.49 \pm 5.72 | 84.71 \pm 0.52 |
| GloGNN++ | 88.33 \pm 1.09 | 77.22 \pm 1.78 | 89.24 \pm 0.39 | 84.05 \pm 4.90 | 37.70 \pm 1.40 | 85.95 \pm 5.10 | 88.04 \pm 3.22 | 85.74 \pm 0.42 |
| PCNet | 88.41 \pm 0.66 | 77.50 \pm 1.06 | 89.51 \pm 0.28 | 88.11 \pm 2.17 | 37.80 \pm 0.64 | 82.16 \pm 2.70 | 88.63 \pm 2.75 | 84.75 \pm 0.51 |
| DirGNN | 86.78 \pm 0.97 | 77.71 \pm 0.78 | 86.94 \pm 0.55 | 76.25 \pm 4.68 | 35.76 \pm 6.31 | 76.51 \pm 6.14 | 80.50 \pm 5.50 | 79.58 \pm 0.75 |
| AxelGNN | 88.18 \pm 1.12 | 77.98 \pm 1.12 | 89.83 \pm 0.66 | 88.36 \pm 5.00 | 39.30 \pm 1.18 | 87.02 \pm 3.49 | 91.25 \pm 2.02 | 86.01 \pm 1.00 |
| AxelGNN _{Sim} | 87.03 \pm 1.04 | 78.25 \pm 1.27 | 88.92 \pm 0.46 | 86.23 \pm 3.75 | 37.64 \pm 1.69 | 84.04 \pm 4.97 | 87.63 \pm 3.60 | 85.98 \pm 0.97 |

Table 4: Node classification accuracy \pm standard deviation (%). The best results are highlighted in **bold**. OOM refers to the out-of-memory.

AxelGNN model performance comparison with base GNNs for the node classification task is shown in Table 4. As per results, AxelGNN consistently outperforms or matches the performance of both traditional and heterophily-aware GNNs. We attribute this to AxelGNN’s ability to model bistable convergence dynamics with heterogeneous relationships between neighbouring nodes, enabling the successful modelling of complex structural connections within both homophilic and heterophilic label patterns. Additionally, AxelGNN_{Sim} also provides comparably solid performance, demonstrating its ability to become an effective and computationally efficient solution for real-world datasets.

6.1.2. Influence Estimation

AxelGNN performance comparison for the influence estimation task is depicted in Table 5. Both AxelGNN variants consistently outperform traditional GNNs, as well as GNNs designed for the influence estimation task. Influence estimation requires the GNN to adapt to the temporal dynamics of the diffusion model. The similarity-gated behaviour of AxelGNN is dynamically changing with each time step, helping AxelGNN variants to mimic the underlying diffusion patterns successfully. Similar to node classification, AxelGNN_{sim} also provides a solid performance for the influence estimation task, demonstrating its strength as an effective and scalable solution.

| | Jazz | | Cora-ML | | Network Science | | Power Grid | |
|------------------------|--------------------------|--------------------------|--------------------------|--------------------------|--------------------------|--------------------------|--------------------------|--------------------------|
| | LT | SIS | LT | SIS | LT | SIS | LT | SIS |
| GCN | 0.199 \pm 0.006 | 0.344 \pm 0.023 | 0.255 \pm 0.008 | 0.365 \pm 0.065 | 0.190 \pm 0.012 | 0.180 \pm 0.007 | 0.335 \pm 0.023 | 0.207 \pm 0.001 |
| GAT | 0.156 \pm 0.100 | 0.288 \pm 0.017 | 0.192 \pm 0.010 | 0.208 \pm 0.008 | 0.114 \pm 0.008 | 0.123 \pm 0.013 | 0.280 \pm 0.015 | 0.133 \pm 0.001 |
| GraphSAGE | 0.120 \pm 0.004 | 0.301 \pm 0.018 | 0.203 \pm 0.009 | 0.222 \pm 0.051 | 0.112 \pm 0.005 | 0.102 \pm 0.010 | 0.341 \pm 0.018 | 0.133 \pm 0.001 |
| DeepIS | 0.219 \pm 0.002 | 0.434 \pm 0.003 | 0.301 \pm 0.005 | 0.304 \pm 0.001 | 0.306 \pm 0.001 | 0.256 \pm 0.001 | 0.374 \pm 0.001 | 0.251 \pm 0.001 |
| DeepIM | 0.134 \pm 0.014 | 0.383 \pm 0.010 | 0.271 \pm 0.010 | 0.270 \pm 0.006 | 0.118 \pm 0.003 | 0.135 \pm 0.004 | 0.331 \pm 0.002 | 0.205 \pm 0.005 |
| GLIE | 0.055 \pm 0.028 | 0.454 \pm 0.062 | 0.286 \pm 0.016 | 0.205 \pm 0.029 | 0.160 \pm 0.003 | 0.103 \pm 0.023 | 0.384 \pm 0.020 | 0.132 \pm 0.026 |
| UniGO | 0.159 \pm 0.020 | 0.335 \pm 0.002 | 0.155 \pm 0.019 | 0.212 \pm 0.001 | 0.110 \pm 0.049 | 0.108 \pm 0.023 | 0.235 \pm 0.005 | 0.206 \pm 0.023 |
| AxelGNN | 0.051 \pm 0.002 | 0.321 \pm 0.006 | 0.144 \pm 0.008 | 0.197 \pm 0.003 | 0.046 \pm 0.002 | 0.100 \pm 0.002 | 0.223 \pm 0.003 | 0.135 \pm 0.004 |
| AxelGNN _{sim} | 0.054 \pm 0.002 | 0.320 \pm 0.006 | 0.152 \pm 0.005 | 0.195 \pm 0.001 | 0.060 \pm 0.003 | 0.103 \pm 0.002 | 0.229 \pm 0.002 | 0.137 \pm 0.001 |

Table 5: Influence estimation MAE \pm standard deviation (%). Lower value indicates better performance. The best results are highlighted in **bold**.

6.2. RQ2: How robust are AxelGNN variants to oversmoothing across different network depths?

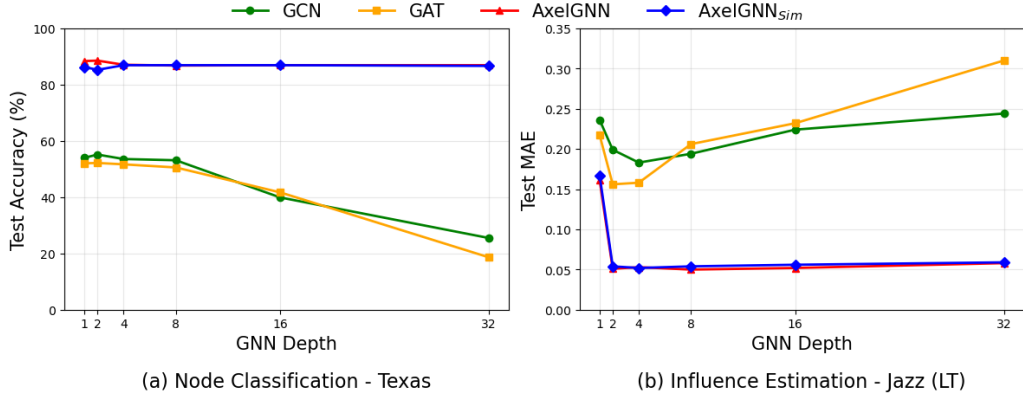


Figure 2: Robustness comparison of AxelGNN variants against oversmoothing across different network depths.

Figure 2 demonstrates the robustness of AxelGNN variants for oversmoothing. For node classification tasks, AxelGNN variants exhibit stable performance across different network depths, while traditional GNNs such as GCN and GAT show significant performance degradation as the number of layers increases. In influence estimation benchmarks, AxelGNN variants consistently maintain low estimation error across varying depths, while conventional GNN architectures experience a substantial increase in estimation error in deeper networks. We attribute this to the global polarization mechanism in our approach that maintains embedding diversity across nodes, effectively preventing the homogenization of node representations.

6.3. *RQ3: What is the impact of hyperparameters on AxelGNN’s performance-efficiency trade-offs?*

We evaluate the performance-efficiency trade-offs of AxelGNN concerning its key hyperparameter, segment size (s), as shown in Figure 3. The results indicate that optimal performance is achieved when the segment size (s) is set to moderate values between 4 and 8. This range strikes an effective balance between model expressiveness and computational efficiency.

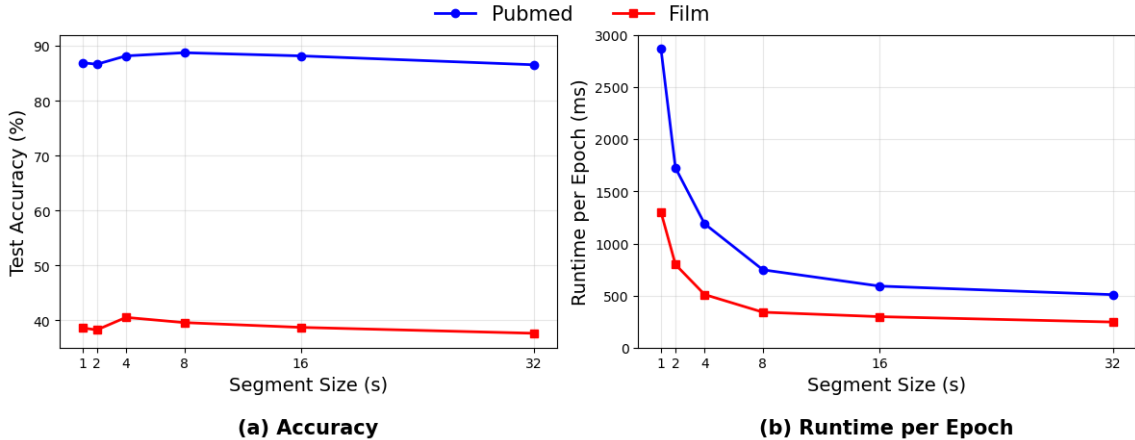


Figure 3: Parameter sensitivity analysis of segment size (s) in AxelGNN across Pubmed and Film datasets.

Using very small values, such as $s = 1$ or 2 , causes the model to become overly granular, treating each feature individually and disrupting important relationships between them that are crucial for learning. This leads to poorer performance. Conversely, when s is too large, like $s = 32$, the copying mechanism becomes excessively broad and combines different types of features, making it difficult for the model to

make precise decisions about which features to copy. This also negatively impacts performance. Overall, this analysis shows that moderate segment sizes provide the best trade-off. They maintain enough granularity for effective feature copying while avoiding the computational burden of excessive fine-grained operations and the loss of expressiveness from overly coarse groupings.

The threshold parameter θ and intensity parameter β are learned automatically during training instead of being manually tuned. These parameters are optimized through backpropagation, adapting to ground truth labels via the downstream loss function. This allows the model to discover optimal interaction dynamics for specific datasets and tasks, with θ determining the similarity threshold for node interactions and β defining the steepness of the interaction probability function.

6.4. RQ4: How do AxelGNN variants exhibit convergence dynamics?

To demonstrate the embedding convergence dynamics of the AxelGNN variants, we plot the mean embedding changes throughout the model learning process on the Citeseer node classification benchmark. The plots are shown in Figure 4.

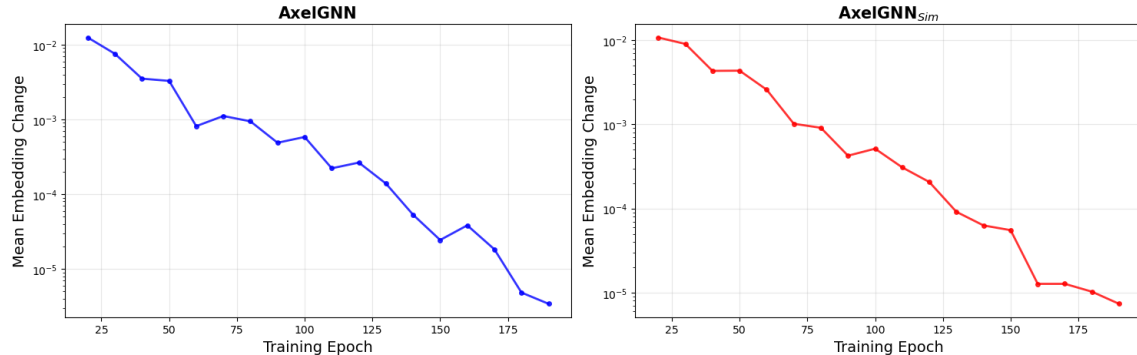


Figure 4: Embedding convergence dynamics of AxelGNN variants.

The exponential decay and subsequent plateau of the curves signify that both models are successfully learning stable representations and achieving embedding convergence. This demonstrates AxelGNN adheres to the theoretical property of convergence in Axelord’s cultural dissemination model. Further, AxelGNN achieves a lower and smoother convergence, indicating a more stable and efficient optimization trajectory compared to the AxelGNN_{sim} variant. This improvement can be attributed to a more detailed and precise parameter design in AxelGNN.

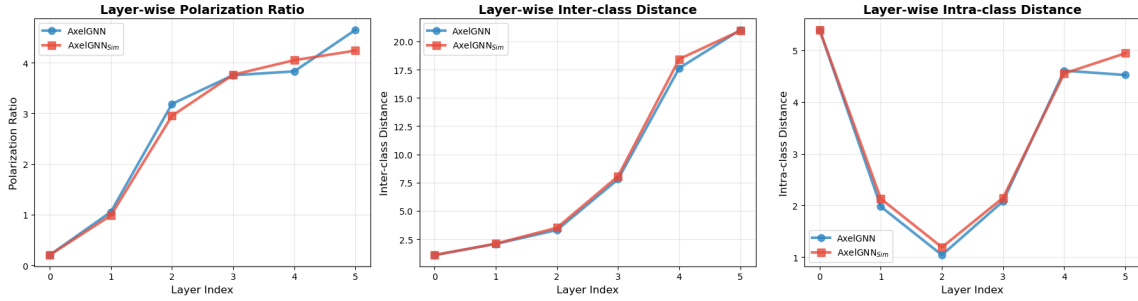


Figure 5: Layer-wise polarization dynamics across network depth for AxelGNN variants.

6.5. RQ5: How do AxelGNN variants exhibit global polarization dynamics across network layers?

To evaluate the global polarization property of AxelGNN variants, we analyze their layer-wise polarization dynamics for node classification on the Citeseer dataset. Figure 5 depicts these dynamics, showing (a) polarization ratio progression (inter-class distance / intra-class distance), (b) inter-class distance evolution, and (c) intra-class distance changes through layers. Both AxelGNN variants exhibit polarization development patterns with the polarization ratio increasing monotonically, indicating progressive class separation. The inter-class distance grows rapidly, indicating node embeddings in different classes would have proper distance separation.

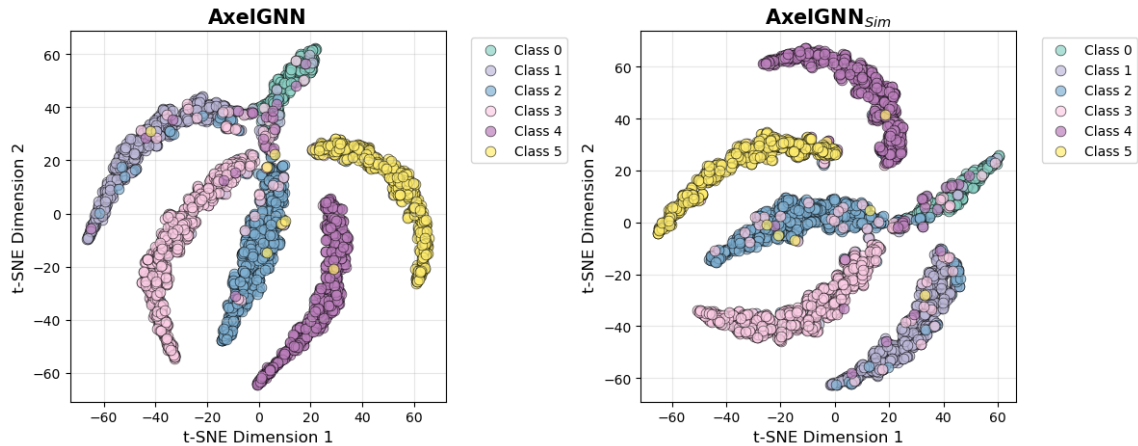


Figure 6: Final embedding space visualization using t-SNE projection for AxelGNN variants.

The t-SNE visualisations of embeddings in Figure 6 reveal successful class separation in both variants. Both achieve comparable cluster separation without inter-class

overlap, suggesting evidence on the ability of AxelGNN variants to achieve global polarization without suffering from oversmoothing.

6.6. RQ6: How robust are AxelGNN variants in maintaining distinct clustering patterns across different network depths?

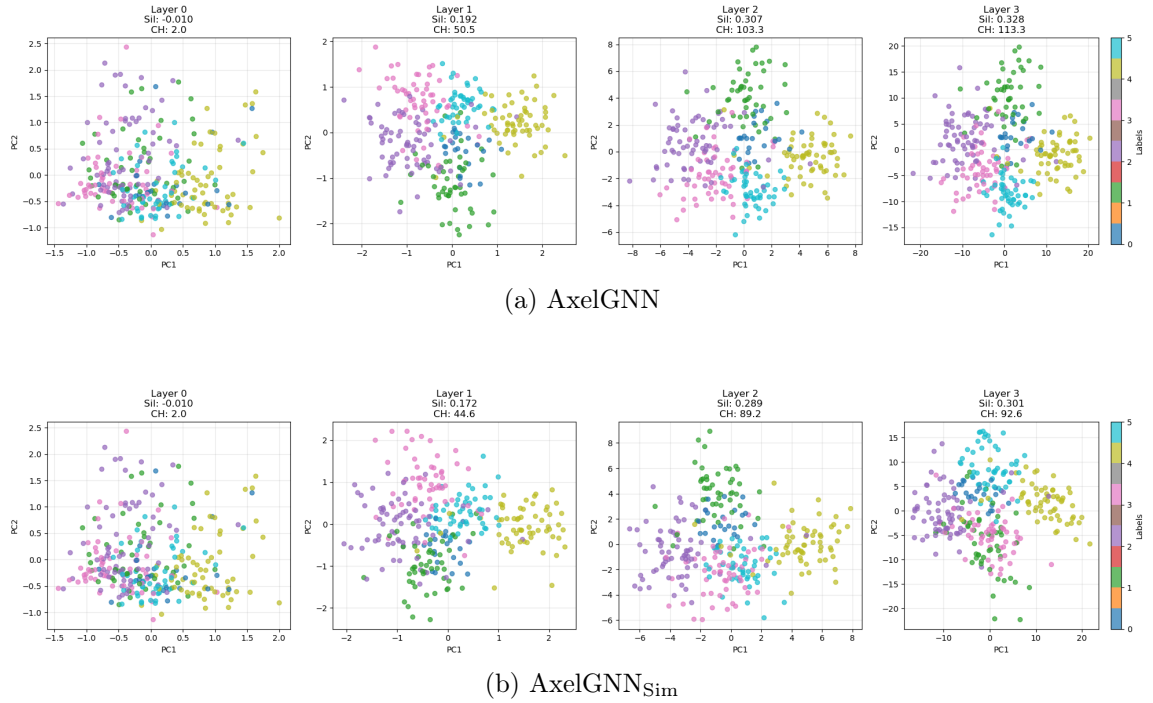


Figure 7: Embedding clustering evolution of AxelGNN variants across layers.

Figure 7 illustrates the evolution of node embeddings across network layers for both AxelGNN variants, where each subplot represents a t-SNE visualisation [62] of the embeddings at different depths on the Citeseer dataset for node classification. The quality of clustering is evaluated using two metrics: the Silhouette (Sil) score [63], which measures the cohesion and separation of clusters (with higher values indicating better-defined clusters), and the Calinski-Harabasz (CH) score [64], which assesses the ratio of between-cluster dispersion to within-cluster dispersion (with higher values indicating more distinct clustering). Both AxelGNN variants demonstrate progressive clustering improvement across network layers. The clustering visualizations reveal distinct behaviors between AxelGNN variants. AxelGNN achieves superior clustering performance, demonstrating well-separated cluster boundaries and aggressive feature transformation. In contrast, AxelGNN_{Sim} shows more conservative

clustering behaviour, producing more compact, densely-packed clusters with reduced inter-cluster distances.

7. Conclusion, Limitations, and Future Work

In this work, we introduce a novel graph neural network architecture called AxelGNN that addresses fundamental limitations in traditional GNNs by incorporating principles from Axelrod’s cultural dissemination model. Our approach successfully tackles three critical challenges: feature oversmoothing, inability to handle heterogeneous relationships, and monolithic feature treatment. AxelGNN adaptively handles both homophilic and heterophilic relationships within a unified framework while maintaining global polarisation to prevent oversmoothing. The proposed trait copying mechanism breaks away from monolithic feature aggregation, allowing fine-grained feature-level interactions that enhance model expressiveness. Our comprehensive experimental evaluation across node classification and influence estimation tasks demonstrates that AxelGNN consistently outperforms or matches state-of-the-art GNN methods across diverse datasets with varying homophily-heterophily characteristics.

Currently, the segment size of AxelGNN is selected as a hyperparameter. While we have provided a parameter sensitivity analysis to determine a feasible value range for this, we plan to learn this value in a data-driven manner. Further, the current approach uses uniform segment sizes across all feature dimensions. Investigating adaptive segmentation strategies that dynamically determine optimal groupings based on feature correlation patterns could further enhance model performance. Beyond these architectural improvements, we plan to evaluate our method on more challenging learning scenarios such as imbalanced classification, out-of-distribution generation, adversarial attacks, and transfer learning. Additionally, we aim to expand our evaluation to other downstream tasks, such as graph classification, graph regression, and link prediction.

Data Availability Statement

All data supporting the findings of this study are publicly available and have been properly cited within the article.

Conflict of Interest

The authors declare that they have no conflict of interest.

References

- [1] Shunxin Xiao, Shiping Wang, Yuanfei Dai, and Wenzhong Guo. Graph neural networks in node classification: survey and evaluation. *Machine Vision and Applications*, 33(1):4, 2022.
- [2] Fan Liang et al. Survey of graph neural networks and applications. *Wireless Communications and Mobile Computing*, 2022(1):9261537, 2022.
- [3] Yandi Li et al. A survey on influence maximization: From an ML-based combinatorial optimization. *ACM Transactions on Knowledge Discovery from Data*, 17(9):1–50, 2023.
- [4] Myriam Jaouadi and Lotfi Ben Romdhane. A survey on influence maximization models. *Expert Systems with Applications*, 248:123429, 2024.
- [5] Muhan Zhang and Yixin Chen. Link prediction based on graph neural networks. In *Advances in Neural Information Processing Systems*, volume 31, 2018.
- [6] Djihad Arrar, Nadjat Kamel, and Abdelaziz Lakhfif. A comprehensive survey of link prediction methods: D. arrar et al. *The Journal of Supercomputing*, 80(3):3902–3942, 2024.
- [7] Stavros Souravlas, Sofia Anastasiadou, and Stefanos Katsavounis. A survey on the recent advances of deep community detection. *Applied Sciences*, 11(16):7179, 2021.
- [8] Xing Su et al. A comprehensive survey on community detection with deep learning. *IEEE Transactions on Neural Networks and Learning Systems*, 35(4):4682–4702, 2022.
- [9] Justin Gilmer, Samuel S Schoenholz, Patrick F Riley, Oriol Vinyals, and George E Dahl. Neural message passing for quantum chemistry. In *Proceedings of the 34th International Conference on Machine Learning*, volume 70 of *ICML*, pages 1263–1272. PMLR, 2017.
- [10] T. Konstantin Rusch, Michael M. Bronstein, and Siddhartha Mishra. A survey on oversmoothing in graph neural networks. Technical Report 2023, SAM Research Report, 2023.
- [11] Wenwen Xia, Yuchen Li, Jun Wu, and Shenghong Li. Deepis: Susceptibility estimation on social networks. In *Proceedings of the 14th ACM International Conference on Web Search and Data Mining*, pages 761–769, 2021.

- [12] Jiong Zhu, Tengfei Ma, Xiang Ma, Bo Li, and Hui Zhao. Beyond homophily in graph neural networks: Current limitations and effective designs. In *Advances in Neural Information Processing Systems*, volume 33, pages 7793–7804, 2020.
- [13] Sitao Luan, Hongzhi Wang, Xiaowei Wu, Junchi Wang, and Yizhou Wang. Revisiting heterophily for graph neural networks. In *Advances in Neural Information Processing Systems*, volume 35, pages 1362–1375, 2022.
- [14] Robert Axelrod. The dissemination of culture: A model with local convergence and global polarization. *Journal of conflict resolution*, 41(2):203–226, 1997.
- [15] Zonghan Wu, Shirui Pan, Fengwen Chen, Guodong Long, Chengqi Zhang, and Philip S Yu. A comprehensive survey on graph neural networks. *IEEE transactions on neural networks and learning systems*, 32(1):4–24, 2020.
- [16] Thomas N Kipf and Max Welling. Semi-supervised classification with graph convolutional networks. In *International Conference on Learning Representations*, 2017.
- [17] Petar Veličković, Guillem Cucurull, Arantxa Casanova, Adriana Romero, Pietro Liò, and Yoshua Bengio. Graph attention networks. In *International Conference on Learning Representations*, 2018.
- [18] Will Hamilton, Zhitao Ying, and Jure Leskovec. Inductive representation learning on large graphs. *Advances in neural information processing systems*, 30, 2017.
- [19] Hongbin Pei, Bingzhe Wei, Kevin Chen Chuan Chang, Yu Lei, and Bo Yang. Geom-gcn: Geometric graph convolutional networks. In *8th International Conference on Learning Representations*, 2020.
- [20] Deyu Bo, Xiao Wang, Chuan Shi, and Huawei Shen. Beyond low-frequency information in graph convolutional networks. In *Proceedings of the AAAI conference on artificial intelligence*, volume 35, pages 3950–3957, 2021.
- [21] Jingwei Guo, Kaizhu Huang, Rui Zhang, and Xinpeng Yi. Es-gnn: Generalizing graph neural networks beyond homophily with edge splitting. *IEEE Transactions on Pattern Analysis and Machine Intelligence*, 2024.
- [22] Ruijia Wang, Shuai Mou, Xiao Wang, Wanpeng Xiao, Qi Ju, Chuan Shi, and Xing Xie. Graph structure estimation neural networks. In *Proceedings of the web conference 2021*, pages 342–353, 2021.

- [23] Tao Wang, Di Jin, Rui Wang, Dongxiao He, and Yuxiao Huang. Powerful graph convolutional networks with adaptive propagation mechanism for homophily and heterophily. In *Proceedings of the AAAI conference on artificial intelligence*, volume 36, pages 4210–4218, 2022.
- [24] Bingheng Li, Erlin Pan, and Zhao Kang. Pc-conv: Unifying homophily and heterophily with two-fold filtering. In *Proceedings of the AAAI conference on artificial intelligence*, volume 38, pages 13437–13445, 2024.
- [25] Dongxiao He, Chundong Liang, Huixin Liu, Mingxiang Wen, Pengfei Jiao, and Zhiyong Feng. Block modeling-guided graph convolutional neural networks. In *Proceedings of the AAAI conference on artificial intelligence*, volume 36, pages 4022–4029, 2022.
- [26] Shuichiro Haruta, Tatsuya Konishi, and Mori Kurokawa. A novel graph aggregation method based on feature distribution around each ego-node for heterophily. In *Asian Conference on Machine Learning*, pages 452–466. PMLR, 2023.
- [27] Yunchong Song, Chenghu Zhou, Xinbing Wang, and Zhouhan Lin. Ordered gnn: Ordering message passing to deal with heterophily and over-smoothing. In *The Eleventh International Conference on Learning Representations*, 2023.
- [28] Shaowei Yin, Yan Yang, Jijie Zhang, and Tianqi Zhou. Adaptive graph convolutional networks based on decouple and residuals to relieve over-smoothing. In *2022 International Joint Conference on Neural Networks (IJCNN)*, pages 01–08. IEEE, 2022.
- [29] Liang Yang, Weihang Peng, Wenmiao Zhou, Bingxin Niu, Junhua Gu, Chuan Wang, Yuanfang Guo, Dongxiao He, and Xiaochun Cao. Difference residual graph neural networks. In *Proceedings of the 30th ACM international conference on multimedia*, pages 3356–3364, 2022.
- [30] Michael Scholkemper, Xinyi Wu, Ali Jadbabaie, and Michael T Schaub. Residual connections and normalization can provably prevent oversmoothing in gnns. In *The Thirteenth International Conference on Learning Representations*, 2025.
- [31] Fei Yang, Huyin Zhang, Shiming Tao, and Sheng Hao. Graph representation learning via simple jumping knowledge networks. *Applied Intelligence*, 52(10):11324–11342, 2022.

- [32] Xiaodong Zhu, Junyu Fu, and Chen Chen. Matrix completion of adaptive jumping graph neural networks for recommendation systems. *IEEE Access*, 11:88433–88450, 2023.
- [33] Dongsheng Luo, Wei Cheng, Wenchao Yu, Bo Zong, Jingchao Ni, Haifeng Chen, and Xiang Zhang. Learning to drop: Robust graph neural network via topological denoising. In *Proceedings of the 14th ACM international conference on web search and data mining*, pages 779–787, 2021.
- [34] Juan Shu, Bowei Xi, Yu Li, Fan Wu, Charles Kamhoua, and Jianzhu Ma. Understanding dropout for graph neural networks. In *companion proceedings of the web conference 2022*, pages 1128–1138, 2022.
- [35] El houssaine Hssayni, Ali Boufssasse, Nour-Eddine Joudar, and Mohamed Eттаouil. Novel dropout approach for mitigating over-smoothing in graph neural networks. *Applied Intelligence*, 55(5):354, 2025.
- [36] Lingxiao Zhao and Leman Akoglu. Pairnorm: Tackling oversmoothing in gnns. In *International Conference on Learning Representations*, 2020.
- [37] Kaixiong Zhou, Xiao Huang, Yuening Li, Daochen Zha, Rui Chen, and Xia Hu. Towards deeper graph neural networks with differentiable group normalization. *Advances in neural information processing systems*, 33:4917–4928, 2020.
- [38] Khang Nguyen, Nong Minh Hieu, Vinh Duc Nguyen, Nhat Ho, Stanley Osher, and Tan Minh Nguyen. Revisiting over-smoothing and over-squashing using ollivier-ricci curvature. In *International Conference on Machine Learning*, pages 25956–25979. PMLR, 2023.
- [39] Yang Liu, Chuan Zhou, Shirui Pan, Jia Wu, Zhao Li, Hongyang Chen, and Peng Zhang. Curvdrop: A ricci curvature based approach to prevent graph neural networks from over-smoothing and over-squashing. In *Proceedings of the ACM Web Conference 2023*, pages 221–230, 2023.
- [40] Lukas Fesser and Melanie Weber. Mitigating over-smoothing and over-squashing using augmentations of forman-ricci curvature. In *Learning on Graphs Conference*, pages 19–1. PMLR, 2024.
- [41] Xu Zhang, Yonghui Xu, Wei He, Wei Guo, and Lizhen Cui. A comprehensive review of the oversmoothing in graph neural networks. In *CCF Conference on Computer Supported Cooperative Work and Social Computing*, pages 451–465. Springer, 2023.

- [42] Zhilin Yang, William Cohen, and Ruslan Salakhudinov. Revisiting semi-supervised learning with graph embeddings. In *International conference on machine learning*, pages 40–48. PMLR, 2016.
- [43] Derek Lim, Felix Hohne, Xiuyu Li, Sijia Linda Huang, Vaishnavi Gupta, Omkar Bhalerao, and Ser Nam Lim. Large scale learning on non-homophilous graphs: New benchmarks and strong simple methods. *Advances in neural information processing systems*, 34:20887–20902, 2021.
- [44] Ryan Rossi and Nesreen Ahmed. The network data repository with interactive graph analytics and visualization. In *Proceedings of the AAAI conference on artificial intelligence*, volume 29, 2015.
- [45] Aleksandar Bojchevski and Stephan Günnemann. Deep gaussian embedding of graphs: Unsupervised inductive learning via ranking. In *International Conference on Learning Representations*, 2018.
- [46] Sami Abu-El-Haija, Bryan Perozzi, Amol Kapoor, Nazanin Alipourfard, Kristina Lerman, Hrayr Harutyunyan, Greg Ver Steeg, and Aram Galstyan. Mixhop: Higher-order graph convolutional architectures via sparsified neighborhood mixing. In *international conference on machine learning*, pages 21–29. PMLR, 2019.
- [47] Ming Chen, Zhewei Wei, Zengfeng Huang, Bolin Ding, and Yaliang Li. Simple and deep graph convolutional networks. In *International conference on machine learning*, pages 1725–1735. PMLR, 2020.
- [48] Susheel Suresh, Vinith Budde, Jennifer Neville, Pan Li, and Jianzhu Ma. Breaking the limit of graph neural networks by improving the assortativity of graphs with local mixing patterns. In *Proceedings of the 27th ACM SIGKDD conference on knowledge discovery & data mining*, pages 1541–1551, 2021.
- [49] Eli Chien, Jianhao Peng, Pan Li, and Olgica Milenkovic. Adaptive universal generalized pagerank graph neural network. In *International Conference on Learning Representations*, 2021.
- [50] Yujun Yan, Milad Hashemi, Kevin Swersky, Yaoqing Yang, and Danai Koutra. Two sides of the same coin: Heterophily and oversmoothing in graph convolutional neural networks. In *2022 IEEE International Conference on Data Mining (ICDM)*, pages 1287–1292. IEEE, 2022.

- [51] Xiang Li, Renyu Zhu, Yao Cheng, Caihua Shan, Siqiang Luo, Dongsheng Li, and Weining Qian. Finding global homophily in graph neural networks when meeting heterophily. In *International conference on machine learning*, pages 13242–13256. PMLR, 2022.
- [52] Emanuele Rossi, Bertrand Charpentier, Francesco Di Giovanni, Fabrizio Frasca, Stephan Günnemann, and Michael M Bronstein. Edge directionality improves learning on heterophilic graphs. In *Learning on graphs conference*, pages 25–1. PMLR, 2024.
- [53] Chen Ling, Junji Jiang, Junxiang Wang, My T Thai, Renhao Xue, James Song, Meikang Qiu, and Liang Zhao. Deep graph representation learning and optimization for influence maximization. In *International conference on machine learning*, pages 21350–21361. PMLR, 2023.
- [54] George Panagopoulos, Nikolaos Tziortziotis, Michalis Vazirgiannis, and Fragkiskos Malliaros. Maximizing influence with graph neural networks. In *Proceedings of the International Conference on Advances in Social Networks Analysis and Mining*, pages 237–244, 2023.
- [55] Hao Li, Hao Jiang, Yuke Zheng, Hao Sun, and Wenying Gong. Unigo: A unified graph neural network for modeling opinion dynamics on graphs. In *Proceedings of the ACM on Web Conference 2025*, pages 530–540, 2025.
- [56] David Kempe, Jon Kleinberg, and Éva Tardos. Maximizing the spread of influence through a social network. In *Proceedings of the ninth ACM SIGKDD international conference on Knowledge discovery and data mining*, pages 137–146, 2003.
- [57] Masahiro Kimura, Kazumi Saito, and Hiroshi Motoda. Efficient estimation of influence functions for sis model on social networks. In *IJCAI*, pages 2046–2051, 2009.
- [58] Petro Liashchynskyi and Pavlo Liashchynskyi. Grid search, random search, genetic algorithm: a big comparison for nas. *arXiv preprint arXiv:1912.06059*, 2019.
- [59] DP Kingma. Adam: a method for stochastic optimization. In *International Conference on Learning Representations*, 2014.
- [60] Michel F Sanner et al. Python: a programming language for software integration and development. *J Mol Graph Model*, 17(1):57–61, 1999.

- [61] Adam Paszke, Sam Gross, Francisco Massa, Adam Lerer, James Bradbury, Gregory Chanan, Trevor Killeen, Zeming Lin, Natalia Gimelshein, Luca Antiga, et al. Pytorch: An imperative style, high-performance deep learning library. *Advances in neural information processing systems*, 32, 2019.
- [62] Laurens van der Maaten and Geoffrey Hinton. Visualizing data using t-sne. *Journal of machine learning research*, 9(Nov):2579–2605, 2008.
- [63] Ketan Rajshekhar Shahapure and Charles Nicholas. Cluster quality analysis using silhouette score. In *2020 IEEE 7th international conference on data science and advanced analytics (DSAA)*, pages 747–748. IEEE, 2020.
- [64] Xu Wang and Yusheng Xu. An improved index for clustering validation based on silhouette index and calinski-harabasz index. In *IOP Conference Series: Materials Science and Engineering*, volume 569, page 052024. IOP Publishing, 2019.